IChemE
www.ingentaselect.com/titles/02638762.htm

0263–8762/04/$30.00+0.00

Trans IChemE, Part A, August 2004
Chemical Engineering Research and Design, 82(A8): 1043–1053

SCALE EFFECTS ON THE HYDRODYNAMICS OF BUBBLE COLUMNS OPERATING IN THE HETEROGENEOUS FLOW REGIME

J. M. VAN BATEN and R. KRISHNA*

Department of Chemical Engineering, University of Amsterdam, Amsterdam, The Netherlands

CFD simulations were carried out in the Eulerian framework using transient three-dimensional strategy in order to describe the influence of column diameter on the hydrodynamics and dispersion characteristics of bubble columns operating in the heterogeneous flow regime. All simulations were carried out with air as the gas phase and water as the liquid phase. A bi-modal distribution of bubble sizes, 'small' and 'large', was assumed for the gas phase. Interactions between the bubbles and the liquid are taken into account by means of a momentum exchange, or drag, coefficient. For small bubbles, the drag coefficient was estimated from experimental data on single bubble terminal velocity. For large bubbles, the drag coefficient is estimated from the experimental data on the large bubble swarm velocity in the limiting case where the superficial gas velocity U approaches the regime transition velocity U_{trans}. The turbulence in the liquid phase is described using the k–ε model. For a bubble column operating at $U = 0.15\ \text{m s}^{-1}$, simulations were carried out for columns of 1, 2, 4, 6 and 10 m in diameter to determine gas holdup, the liquid circulation velocity, and the axial dispersion coefficient of the liquid phase, $D_{\text{ax,L}}$, and that of the large and small bubble phases. The results demonstrate the strong increase of liquid circulations, and $D_{\text{ax,L}}$ with increasing column diameter. The dispersion of the small bubbles has the same order of magnitude as that of $D_{\text{ax,L}}$.

Keywords: bubble columns; heterogeneous flow regime; CFD; scale effects regime transition; axial dispersion.

INTRODUCTION

Bubble columns are widely used in industry for carrying out a variety of chemical reactions such as hydrogenations, oxidations and the Fischer Tropsch synthesis. Many recent experimental studies have emphasized the strong influence of column diameter on bubble column hydrodynamics operating in the heterogeneous flow regime (Forret *et al.*, 2003; Krishna *et al.*, 1999a). In particular, the strength of the liquid circulations increases significantly with increasing column diameter, and as a consequence the liquid phase tends to approach well-mixed conditions. The liquid circulations tend to accelerate the bubbles travelling upward in the central core. When the bubbles disengage at the top of the dispersion, the liquid travels back down the wall region. The bubble rise velocity, and consequently the gas holdup, is therefore a function of the reactor diameter (Krishna and van Baten, 2002; Krishna *et al.*, 2001). Clearly, to describe the influence of liquid circulations on the gas holdup, we need to be able to predict the liquid circulation velocity as a function of the superficial gas velocity, U, and column diameter, D_{T}. One measure of the liquid circulations is the axial component of the velocity of the liquid at the central axis of the column, $V_{\text{L}}(0)$. Figure 1(a) shows published data (Forret *et al.*, 2003; Krishna *et al.*, 1999a) on $V_{\text{L}}(0)$ for air–water systems for D_{T} in the range 0.1–1 m. Also shown in Figure 1(a) are the literature correlations for $V_{\text{L}}(0)$ of Riquarts (1981):

$$V_{\text{L}}(0) = 0.21(gD_{\text{T}})^{1/2}\left(\frac{U^3\rho_L}{g\mu_{\text{L}}}\right)^{1/8} \tag{1}$$

and Zehner (1986):

$$V_{\text{L}}(0) = 0.737(UgD_{\text{T}})^{1/3} \tag{2}$$

The major uncertainty in extrapolating to say $D_{\text{T}} = 10$ m is self evident, especially in view of the fact that there are no experimental data for columns larger than 1 m in diameter. In this connection it must be remarked that the experimental work of Koide *et al.* (1979) and Kojima *et al.* (1980), carried out in a 5.5 m diameter column, is not usable for our purposes because the operation was restricted to superficial gas velocities below $0.05\ \text{m s}^{-1}$. The focus of the work in

**Correspondence to*: Professor R. Krishna, Department of Chemical Engineering, University of Amsterdam, Nieuwe Achtergracht 166, 1018 WV Amsterdam, The Netherlands.
E-mail: r.krishna@uva.nl

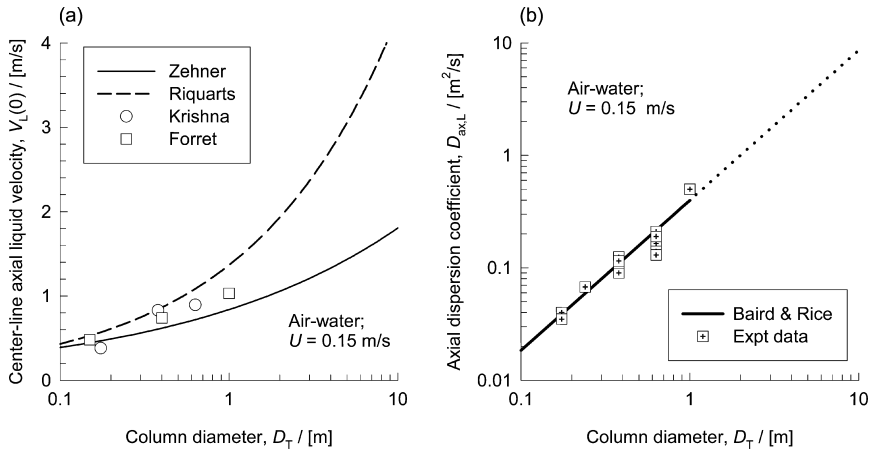

Figure 1. (a) Centre-line liquid velocity $V_L(0)$ for air–water bubble columns as a function of column diameter D_T. (b) Liquid phase axial dispersion coefficient $D_{ax,L}$ for air–water bubble columns as a function of column diameter D_T. Also plotted are the experimental data of Forret *et al.* (2003) and Krishna *et al.* (1999a).

this paper is the heterogeneous flow regime, with superficial gas velocities well in excess of 0.05 m s^{-1}.

With increasing liquid circulations, the dispersion (backmixing) in the liquid phase increases. Figure 1(b) shows measured data (Forret *et al.*, 2003; Krishna *et al.*, 2000a) on $D_{ax,L}$ for the air–water system for D_T in the range 0.1–1 m, operating at $U = 0.15$ m s^{-1}. Also shown in Figure 1(b) is the Baird and Rice (1975) correlation for $D_{ax,L}$:

$$D_{ax,L} = 0.35 D_T^{4/3} (gU)^{1/3} \tag{3}$$

The applicability of the Baird–Rice correlation for estimation of $D_{ax,L}$ for a bubble column reactor of say 10 m diameter is open to question, as the database used for setting up the correlation consisted of experiments in columns smaller than 1 m in diameter.

Several recent publications have established the potential of computational fluid dynamics (CFD) in the Eulerian framework for describing the hydrodynamics of bubble columns (Jakobsen *et al.*, 1997; Joshi, 2001; Krishna *et al.*, 1999a, 2000b; Krishna and Van Baten, 2001b; Pan *et al.*, 1999; Sanyal *et al.*, 1999; Sokolichin and Eigenberger, 1999). The major objective of the present work is to use the Eulerian simulation strategy for obtaining information on gas holdup, liquid circulations and liquid dispersion for a bubble column reactor with the air–water system in columns larger than 1 m diameter operating in the heterogeneous flow regime. The second objective is to examine the extent to which the literature correlations for $V_L(0)$ and $D_{ax,L}$ are adequate to describe the hydrodynamics.

DEVELOPMENT OF EULERIAN SIMULATION MODEL

Our approach for modelling purposes is to assume that in the heterogeneous flow regime we have two distinct bubble classes: 'small' and 'large'; see Figure 2. The small bubbles are either spherical or ellipsoidal in shape depending the physical properties of the liquid (Clift *et al.*, 1978). The large bubbles fall into the spherical cap regime. In conformity with the model of Krishna and Ellenberger (1996), we assume that the superficial gas velocity through the small bubble phase corresponds to that at the regime transition point, U_{trans}. The transition velocity can be estimated using the Reilly *et al.* (1994) correlation, or can be provided as model input.

For each of the three phases shown in Figure 2 the volume-averaged mass and momentum conservation equations in the Eulerian framework are given by:

$$\frac{\partial(\varepsilon_k \rho_k)}{\partial t} + \nabla \cdot (\rho_k \varepsilon_k \mathbf{u}_k) = 0 \tag{4}$$

$$\frac{\partial(\rho_k \varepsilon_k \mathbf{u}_k)}{\partial t} + \nabla \cdot (\rho_k \varepsilon_k \mathbf{u}_k \mathbf{u}_k) = \mu_{k,\text{eff}} \varepsilon_k \left[\nabla \mathbf{u}_k + (\nabla \mathbf{u}_k)^T\right] - \varepsilon_k \nabla p + \mathbf{M}_{kl} + \rho_k \varepsilon_k \mathbf{g} \tag{5}$$

where, ρ_k, $\mathbf{u}_k$ and ε_k represent, respectively, the macroscopic density, velocity and volume fraction of phase k; $\mu_{k,\text{eff}}$ is the effective viscosity of the fluid phase k, including the molecular and turbulent contributions, $\mu_{k,\text{eff}} = \mu_k + \mu_{k,\text{turb}}$, p is the pressure, $\mathbf{M}_{kl}$, the interphase momentum exchange between phase k and phase l and $\mathbf{g}$ is the gravitational acceleration.

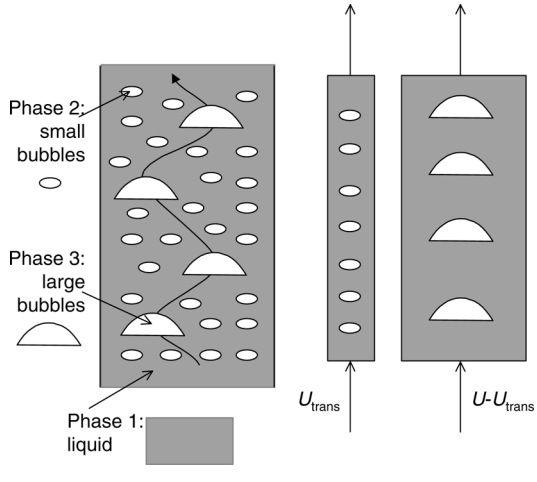

Figure 2. Model for bubble columns operating in the heterogeneous flow regime.

The momentum exchange between either bubble phase (subscript b) and liquid phase (subscript L) phases is given by

$$\mathbf{M}_{\mathrm{L,b}} = \left[\frac{3}{4}\frac{C_{\mathrm{D}}}{d_{\mathrm{b}}}\rho_{\mathrm{L}}\right]\varepsilon_{\mathrm{b}}\varepsilon_{\mathrm{L}}\left(\mathbf{u}_{\mathrm{b}} - \mathbf{u}_{\mathrm{L}}\right)\left|\mathbf{u}_{\mathrm{b}} - \mathbf{u}_{\mathrm{L}}\right| \tag{6}$$

where we follow the formulation given by Pan *et al.* (1999). The inclusion of ε_{L} in equation (6) is to avoid computational problems that potentially arise in the 'gas cap' above the dispersion layer in the column. Inclusion of ε_{L} ensures that, in regions where the liquid holdup is zero (say in the gas cap), there is no momentum exchange between the gas and liquid phases. This condition is not met if only gas holdup is present in the momentum exchange term and, as a result, the liquid will experience an unrealistically high drag at very high gas volume fractions. The liquid phase exchanges momentum with both the 'small' and 'large' bubble phases. No interchange between the 'small' and 'large' bubble phases has been included in the present model and each of the dispersed bubble phases exchanges momentum only with the liquid phase. Many authors (Hagesaether *et al.*, 2002a, b; Luo and Svendsen, 1996) have stressed the importance of bubble breakage and coalescence, especially in the distributor zone. Indeed, in describing gas–liquid mass transfer in bubble columns, it is essential to consider coalescence and breakup phenomena (De Swart *et al.*, 1996; Krishna and van Baten, 2003). In the current paper we focus on the hydrodynamics aspects and interactions between large and small bubbles can be ignored provided the time-averaged gas holdups are not influenced. We have only included the drag force contribution to $\mathbf{M}_{\mathrm{L,b}}$, in keeping with the works of Sanyal *et al.* (1999) and Sokolichin and Eigenberger (1999). The added mass and lift force contributions were both ignored in the present analysis. In the churn-turbulent regime of operation both these forces are expected to be of negligible importance compared with the drag force.

For a swarm of bubbles, either small or large, rising in a gravitational field, the drag force balances the differences between the weight and buoyancy and so the square bracketed term in equation (6) containing the drag coefficient C_{D} becomes (Clift *et al.*, 1978):

$$\frac{3}{4}\frac{C_{\mathrm{D}}}{d_{\mathrm{b}}}\rho_{\mathrm{L}} = (\rho_{\mathrm{L}} - \rho_{\mathrm{G}})g\frac{1}{V_{\mathrm{b0}}^2} \tag{7}$$

where V_{b0} is the rise velocity of the bubble swarm in the limit of vanishing superficial gas velocity. When the superficial gas velocity U is increased, liquid circulations are induced and equation (6) will properly take account of the slip between the bubble and liquid phases.

For 'small' bubbles rising in an air–water bubble column, the rise velocity V_{b0} is practically independent of the bubble size in the 3–8 mm range; see the experimental data (Krishna *et al.*, 1999b) presented in Figure 3. For the 'small' bubbles the term

$$\left[\frac{3}{4}\frac{C_{\mathrm{D}}}{d_{\mathrm{b}}}\rho_{\mathrm{L}}\right]$$

is estimated from equation (7) taking $V_{\mathrm{b0}} = 0.23\ \mathrm{m\,s^{-1}}$.

For a swarm of 'large' bubbles, experimental data (Krishna and Van Baten, 2001b) for air–water systems in columns of 0.1, 0.19 and 0.38 m diameter show that V_{b0} has a value of $1\ \mathrm{m\,s^{-1}}$ in the limit of low superficial gas velocity

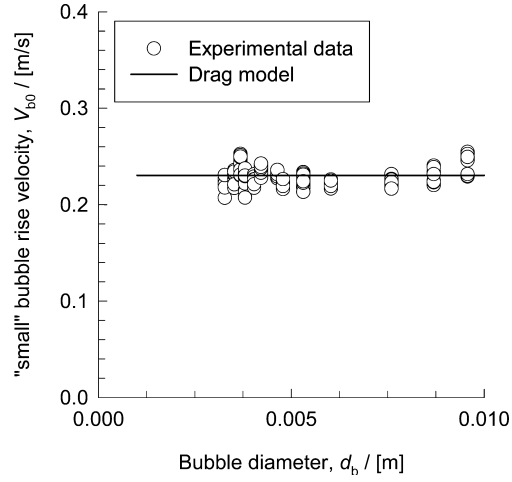

Figure 3. Experimental data on rise velocity of 'small' bubbles in water as a function of bubble diameter (Krishna *et al.*, 1999b).

through the large bubbles, $(U - U_{\mathrm{trans}})$; see Figure 4. The large bubble rise velocity of $V_{\mathrm{b0}} = 1\ \mathrm{m\,s^{-1}}$ is only slightly higher than the rise velocity of a single spherical cap bubble of 0.08 m diameter in stagnant water (Krishna *et al.*, 1999b). For the 'large' bubbles the term

$$\left[\frac{3}{4}\frac{C_{\mathrm{D}}}{d_{\mathrm{b}}}\rho_{\mathrm{L}}\right]$$

is estimated from equation (7) taking $V_{\mathrm{b0}} = 1\ \mathrm{m\,s^{-1}}$. With increasing superficial gas velocity, and column diameter, the liquid circulations are enhanced and the large bubbles will be accelerated; this effect is automatically accounted for in equation (6).

For the continuous, liquid (water), phase, the turbulent contribution to the stress tensor is evaluated by means of k–ε model, using standard single phase parameters $C_{\mu} = 0.09$, $C_{1\varepsilon} = 1.44$, $C_{2\varepsilon} = 1.92$, $\sigma_k = 1$ and $\sigma_{\varepsilon} = 1.3$. In the k–ε model $\mu_{\mathrm{turb}} = C_{\mu}\rho k/\varepsilon^2$. The applicability of the k–ε model has been considered in detail by Sokolichin and Eigenberger (1999). No turbulence model is used for calculating the velocity fields of the dispersed bubble phases.

A commercial CFD package CFX 4.4, of ANSYS Inc., Canonsburg, USA, was used to solve the equations of continuity and momentum. This package is a finite volume solver, using body-fitted grids. The grids are non-staggered and all variables are evaluated at the cell centres. An improved version of the Rhie and Chow (1983) algorithm is used to calculate the velocity at the cell faces. The pressure-velocity coupling is obtained using the SIMPLEC algorithm (van Doormal and Raithby, 1984). For the convective terms in equations (4) and (5) hybrid differencing was used. A fully implicit backward differencing scheme was used for the time integration.

From the Reilly *et al.* (1994) correlation it was determined that the superficial gas velocity at the regime transition point for air–water $U_{\mathrm{trans}} = 0.034\ \mathrm{m\,s^{-1}}$. This value is taken to hold for columns with diameters ranging from 1 to 10 m. Since the simulation results presented below are for $U = 0.15\ \mathrm{m\,s^{-1}}$, small uncertainties in the estimation of U_{trans} are not expected to be crucial. Following the model of Krishna and Ellenberger (1996), we assume that in the

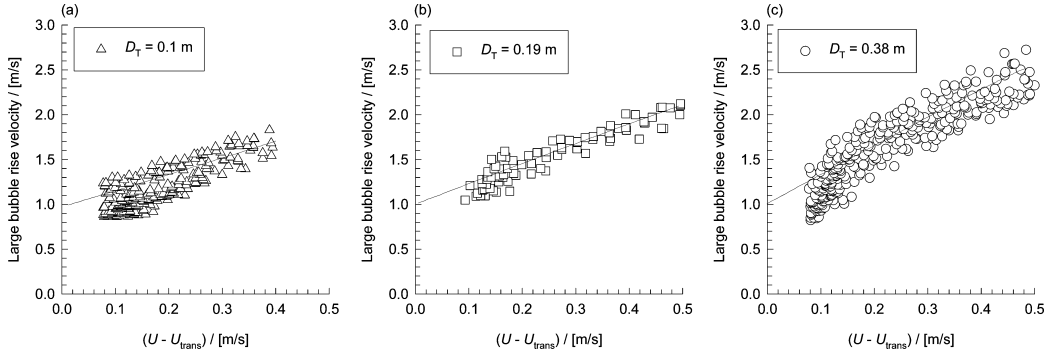

Figure 4. Experimental data on rise velocity of 'large' bubble swarms in water as a function of superficial gas velocity through the large bubbles ($U - U_{trans}$) for columns of 0.1, 0.19 and 0.38 m diameter. The data is from Figure 25 of Krishna and van Baten (2001). (a) Large bubble swarm in 0.1 m column; (b) large bubble swarm in 0.19 m column; (c) large bubble swarm in 0.38 m column.

churn-turbulent flow regime the superficial gas velocity through the small bubble phase is $U_{trans} = 0.034\,m\,s^{-1}$ (see Figure 2). The remainder of the gas ($U - U_{trans}$) was taken to rise up the column in the form of large bubbles. This implies that at the distributor the 'large' bubbles constitute a fraction $(U - U_{trans})/U$ of the total incoming volumetric flow, whereas the 'small' bubble constitute a fraction (U_{trans}/U) of the total incoming flow. The small bubbles were injected at the inner 80% cells in the bottom patch. The large bubbles were injected at the inner 60% cells of the bottom patch. We also confirmed that the simulation results were not significantly altered if the large bubbles were to be injected over 80% of the bottom patch. The outer peripheral region of the distributor was not aerated.

A pressure boundary condition was applied to the top of the column. A standard wall function is applied for turbulent quantities and velocities near the wall. The boundary value for velocity at the wall is zero (no-slip). There is no flux of volume fraction through the walls; the spatial derivative of volume fraction perpendicular to the wall is zero (volume fraction is not zero in the first cell, next to the wall, inside the computational domain). The physical properties of the gas and liquid phases are specified in Table 1. The details of the operating conditions and computational grids used in the various campaigns are specified in Table 2. For any simulation, the column was filled with liquid up to a certain height (as specified in Table 2) and at time zero the gas velocity was set at the specified value U at the bottom face.

Typical time stepping strategy used was: 100 steps at 5×10^{-5} s, 100 steps at 1×10^{-4} s, 100 steps at 5×10^{-4} s, 100 steps at 1×10^{-3} s, 200 steps at 3×10^{-3} s, 1400 steps at 5×10^{-3} s, and all remaining steps were set at 1×10^{-2} s until quasi-steady state was obtained. Quasi-steady state in the transient simulations was indicated by a situation in which all of the variables varied around a constant average value for a sufficiently long time period, usually 100 s.

Table 1. Physical properties of phases used in CFD simulations.

	Liquid (water)	Gas (air)
Viscosity, μ (Pa s)	1×10^{-3}	1.7×10^{-5}
Density, ρ (kg m^{-3})	998	1.3
Diffusivity of tracer, $Đ$ (m^2 s^{-1})	1×10^{-9}	1×10^{-5}

To estimate the liquid phase axial dispersion, the final state of a hydrodynamics run was used to start a dynamic run in which a mass tracer is injected into the liquid phase near the top of the dispersion. In keeping with experimental studies on tracer injection, the properties of the tracer were taken to be identical to that of the liquid phase. Tracer 'addition' only amounts to changing the mass fraction of the tracer at the point of the tracer injection at the specified location. There is no increase in the mass of the system at the time of tracer injection. The concentration of the mass tracer was monitored at three heights along the column, following a simulation technique described in earlier work (van Baten and Krishna, 2001). The following equations are solved for the mass tracer:

$$\frac{\partial}{\partial t}\varepsilon_k \rho_k C_k + \nabla \cdot \left(\varepsilon_k \rho_k \mathbf{u}_k C_k - Đ_k \varepsilon_k \rho \nabla C_k\right) = 0 \qquad (8)$$

Here, C_k is the concentration of mass-tracer in phase k and $Đ_k$ is the diffusion coefficient of mass tracer in phase k (listed in Table 1). Since there is zero liquid throughput (liquid operates in batch), eventually all mass tracer gets distributed equally along the liquid phase. For the mass tracer simulations, some smaller time steps were used to guarantee a smooth restart from the hydrodynamics run, and then time steps of 1×10^{-2} s were used.

The liquid phase axial dispersion coefficient was determined by a least-squares fit of the liquid-phase RTD curves at a distance L_i from the point of tracer injection (Deckwer, 1992):

$$\frac{C_L(x,t)}{C_{L,0}} = 1 + 2\sum_{n=1}^{\infty} \cos\left(\frac{n\pi L_i}{L}\right) \exp\left[-D_{ax,L}\left(\frac{\pi n}{L}\right)^2 t\right]; \quad i = 1,2,3 \qquad (9)$$

Here, L is the total height of the dispersion, t is time and L_1, L_2 and L_3 are distances from the point of tracer injection along the dispersion height to the three monitoring stations (see Figure 5). An upper limit of $n = 20$ rather than infinity was found to be sufficiently accurate for the summation. The reference concentration $C_{L,0}$ was determined by the average concentration of all observation points at the end of the RTD simulation.

Additionally, the gas phase (small and large bubbles) entering the column at the bottom was also traced and the tracer concentrations monitored at station 1 for the small and large bubble phase, separately.

Table 2. Details of three-dimensional simulation campaign.

Column diameter, D_T (m)	Superficial gas velocity, U (m s^{-1})	Column height, H_T (m)	Observation height for hydro-dynamics, H_{obs} (m)	Initial height of liquid in the column, H_0 (m)	Cells in radius	Cells in height	Cells in azimuthal direction	Total number of cells	Number of days to complete hydro-dynamics and RTD (each run)
1	0.08, 0.11, 0.15, 0.19	7.0	4.5	4.65	20	140	10	28,000	15
2.0	0.15	14.0	6.0	9.3	30	210	10	63,000	25
4.0	0.15	28.0	14.4	18.64	40	350	10	140,000	60
6.0	0.15	42.0	24.0	28.0	50	420	10	210,000	100
10.0	0.15	42.0	24.0	28.0	50	420	10	210,000	100

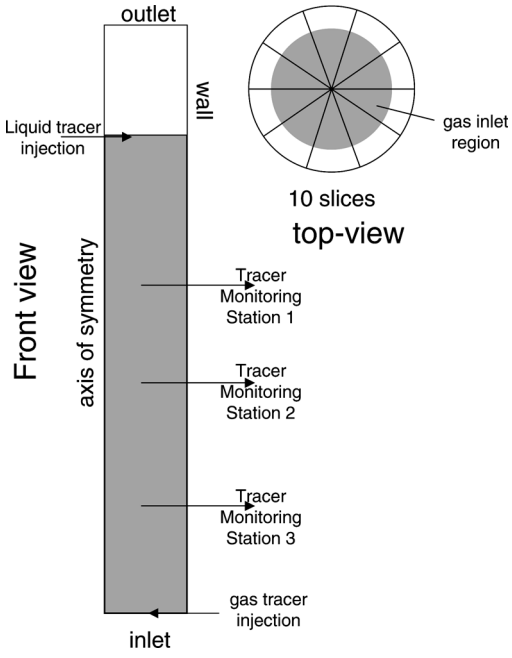

Figure 5. Schematic showing the computational domain and the tracer injection and monitoring stations to determine $D_{ax,L}$.

Two sorts of campaigns were carried out. Firstly, for a column of 1 m diameter, simulations were carried out for $U = 0.08$, 0.11, 0.15 and 0.19 m s^{-1}, in order to validate the CFD simulations by comparing with the experiments of Forret *et al.* (2003). In the second campaign, the superficial gas velocity was kept constant at $U = 0.15$ m s^{-1} and the column diameters were varied: $D_T = 1$, 2, 4, 6 and 10 m. All simulations were carried out on a set of five PC Linux workstations, each equipped with a single Pentium 4 processor. The approximate time required to complete the hydrodynamic and the RTD runs are shown in Table 2. For example, a single campaign at $U = 0.15$ m s^{-1} on the 10 m diameter took more than 3 months to produce the hydrodynamics and RTD information. Further details of the simulations, including animations of column start-up dynamics are available on our web site: http://ct-cr4.chem.uva.nl/AWScaleUp/.

RESULTS AND DISCUSSION

Let us consider the results of the simulation campaign for the 1 m diameter column, with varying superficial gas velocity U. The dynamic behaviour of the centre-line liquid velocity $V_L(0)$ is shown in Figure 6 and emphasize the inherently chaotic behaviour, with liquid sloshing from side to side; these effects, which are in conformity with visual observations, can best be appreciated by viewing the animations on our website: http://ct-cr4.chem.uva.nl/AWScaleUp/. The transient simulations were run for sufficiently long period of time and the hydrodynamic parameters such as ε and $V_L(0)$ were determined by averaging over the time period where quasi-steady state prevails. Quasi-steady state is assumed to prevail when the mean value of $V_L(0)$ is practically time invariant. Figure 7 shows the $V_L(0)$ values as a function of U. The error bars in the $V_L(0)$ for the CFD simulations shown in Figure 7 represent the standard deviations obtained from the transient $V_L(0)$ dynamics in Figure 6. The experimental data (Forret *et al.*, 2003) of $V_L(0)$ at $U = 0.15$ m s^{-1} is in reasonable agreement with the corresponding CFD simulation result. From Figure 7 we may also conclude that the Zehner correlation (2) is to be preferred to the Riquarts (1) correlation in order to describe the dependence of $V_L(0)$ on the superficial gas velocity.

Figure 8(a) shows the radial distribution of the axial component of the liquid velocity $V_L(r)$ obtained from CFD simulations for $D_T = 1$ m and $U = 0.15$ m s^{-1}. This distribution represents the values at the observation height specified in Table 2. Also, shown in Figure 8(a) is the experimental data of Forret *et al.* (2003). The agreement between CFD and experiment is reasonably good.

Figure 8(b) shows the radial distribution of the gas holdup of 'small' and 'large' bubbles for $D_T = 1$ m and $U = 0.15$ m s^{-1}. We see that the large bubbles tend to concentrate in the central core of the column whereas the small bubbles predominate in the outer periphery of the column. The cross-sectional area average total gas holdup, $\varepsilon = 0.244$, which is in excellent agreement with the value of 0.24 reported by Forret *et al.* (2003).

Let us now consider the dynamic behaviour of the axial component of the liquid velocity, $V_L(0)$ (monitored at the observation heights, H_{obs}, specified in Table 2) for operation at $U = 0.15$ m s^{-1} for various column diameters (see Figure 9). It is apparent that with increasing scale both the magnitude of $V_L(0)$, and its fluctuation around the mean increases. The hydrodynamic parameters were obtained by averaging over the time period during which quasi-steady state can be assumed to prevail. These time-averaged values of $V_L(0)$ are shown in Figure 10(a), in which the error bars represent the standard deviations of the velocity fluctuations shown in Figure 9. The $V_L(0)$ values, which

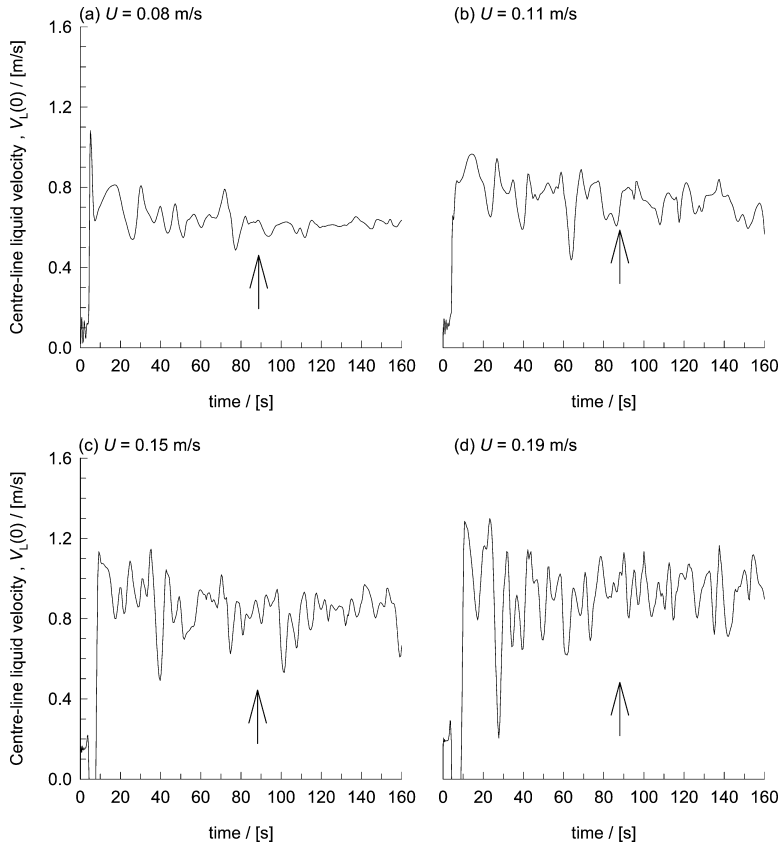

Figure 6. Transient approach to quasi-steady state for 1 m diameter column, operating at $U = 0.08$, 0.11, 0.15 and 0.19 m s^{-1}. The arrows represent the time of injection of tracer in three-dimensional simulations for determination of the liquid phase dispersion coefficient. Animations of column start-up dynamics are available on our web site: http://ct-cr4.chem.uva.nl/AWScaleUp/.

increase with scale, appear to follow the trend predicted by the Zehner (1986) correlation. The Zehner correlation (2) is clearly superior to the Riquarts (1) correlation for describing the column diameter dependence of $V_L(0)$.

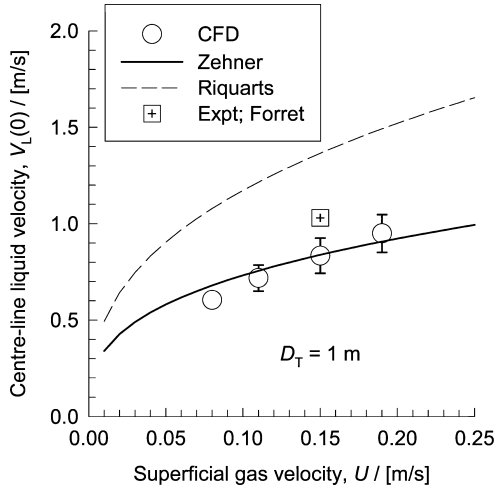

Figure 7. Data on centre-line liquid velocity $V_L(0)$ in 1 m diameter column as function of U. The experimental data (Forret *et al.*, 2003) are compared with three-dimensional simulation results. The error bars on the three-dimensional simulation data represent the standard deviations of the transient $V_L(0)$ data presented in Figure 6, obtained from the data set after the time indicated by the arrow mark.

When the liquid velocity profiles obtained from the CFD simulations are normalized with respect to the centre-line velocity, the $V_L(r)/V_L(0)$ are practically independent of the column diameter. This is illustrated in Figure 8(c) for the three-dimensional simulation campaign at $U = 0.15$ m s^{-1} for various column diameters up to 10 m. The significance of the result portrayed in Figure 8(c) is that the centre-line velocity $V_L(0)$ can be taken to be a unique measure of the strength of liquid circulations.

An important consequence of the fact that the strength of the liquid circulations increases with increasing scale is that the gas holdup values are correspondingly lowered; this is shown in Figure 10(b). We note that the gas holdup in the 10 m diameter reactor is 0.16, whereas for the 1 m column the value of $\varepsilon = 0.24$. A 20% decrease in gas holdup with increase of scale can have significant consequences for a reactor designed for high conversion targets.

A tracer is injected into the liquid phase near the top of the liquid dispersion, at the time step indicated by an arrow in Figure 9 and the progression of this tracer is monitored at three stations along the height of the column (see Figure 5). As explained earlier the tracer 'addition' essentially amounts to setting the mass fraction of tracer to unity (arbitrary units) at a specified location near the top of the dispersion. The CFD simulations of the tracer RTD is then fitted with the model given by equation (9). Typical results comparison of the dimensionless RTD curves for the tracer are shown in Figure 11 for $D_T = 1$, 2, 4 and 6 m, operating at $U = 0.15$ m s^{-1}. We note from Figure 11 that the tracer

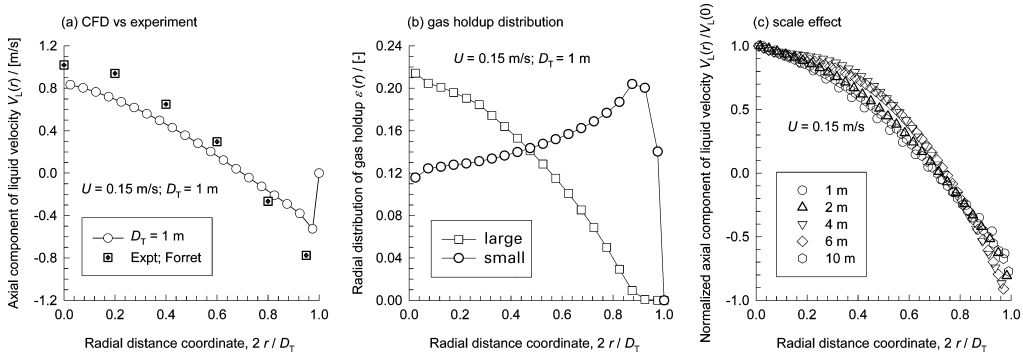

Figure 8. (a) Radial distribution of the axial component of liquid velocity $V_L(r)$ for operation at $U = 0.15\,\mathrm{m\,s^{-1}}$ in 1 m diameter column. The CFD simulations are compared with the experimental data of Forret *et al.* (2003). (b) Radial distribution of holdup of 'small' and 'large' bubbles for operation at $U = 0.15\,\mathrm{m\,s^{-1}}$ in 1 m diameter column. (c) Radial distribution of the normalized axial component of liquid velocity $V_L(r)/V_L(0)$ for operation at $U = 0.15\,\mathrm{m\,s^{-1}}$ from three-dimensional simulations of 1, 2, 4, 6 and 10 m columns.

response is not smooth but oscillates. These oscillations are due to liquid sloshing from side to side causing a significant radial transport of the liquid tracer, as can be witnessed in the animations on our web site: http://ct-cr4.chem.uva.nl/AWScaleUp/. In this context it is worth emphasizing that two-dimensional axi-symmetric simulations will yield a much lower value of $D_{ax,L}$ than three-dimensional simulations because there is no mechanism for radial transport (van Baten and Krishna, 2001).

Each of the tracer curves, such as those shown in Figure 11 were fitted individually to obtain three different values of $D_{ax,L}$ for each run. Figure 12 shows the results for the two campaigns with (a) varying U for $D_T = 1$ m and (b) varying D_T for $U = 0.15\,\mathrm{m\,s^{-1}}$. Also plotted in Figure 12(b) are the experimentally determined $D_{ax,L}$ values for the air–water system culled from the literature for operation at $U = 0.15\,\mathrm{m\,s^{-1}}$ (Forret *et al.*, 2003; Krishna *et al.*, 2000a). From Figure 12 it can be seen that the both the Baird and Rice correlation (3) and CFD simulations show similar *trends* in the dependence of $D_{ax,L}$ on U and D_T. The CFD simulations, however, predict slightly lower values for $D_{ax,L}$.

The response to the gas tracer experiment in the 1, 2, 4, 6 and 10 m diameter columns ($U = 0.15\,\mathrm{m\,s^{-1}}$), monitored at station 1 are shown in Figure 13 for large and small bubbles, separately. From a practical point of view the large bubbles could be assumed to rise through the column virtually in plug flow. The RTD curve of the small bubbles shows a long tail, signifying a high degree of dispersion. We also note that

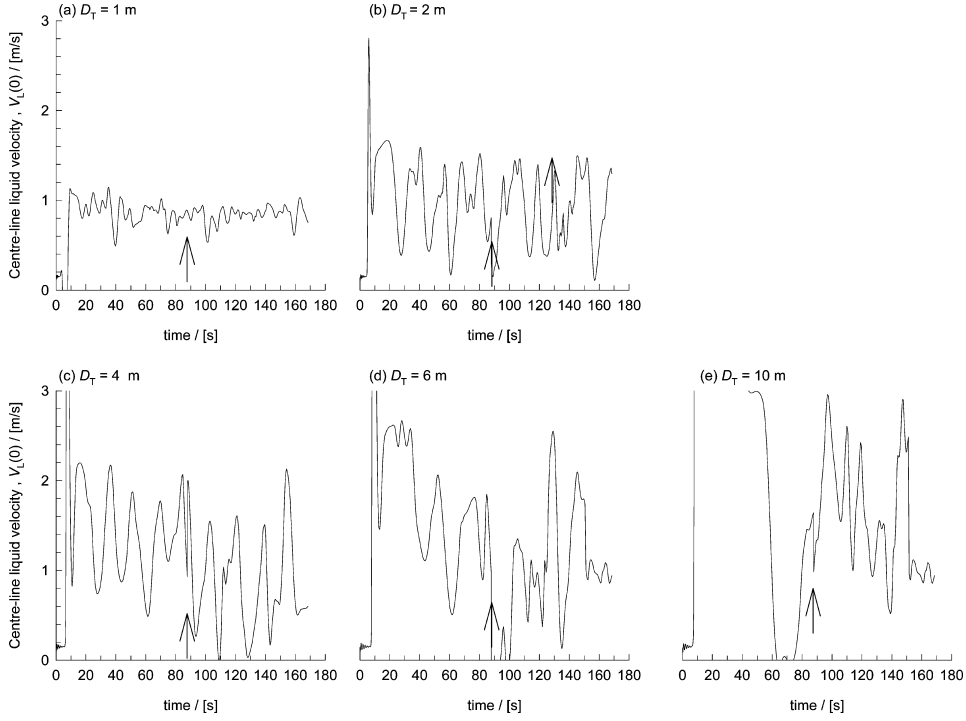

Figure 9. Transient approach to quasi-steady state (three-dimensional) for operation at $U = 0.15\,\mathrm{m\,s^{-1}}$ in columns of 1, 2, 4, 6 and 10 m diameter. The arrows represent the time of injection of tracer in three-dimensional simulations for determination of the liquid phase dispersion coefficient. Animations of column start-up dynamics are available on our web site: http://ct-cr4.chem.uva.nl/AWScaleUp/.

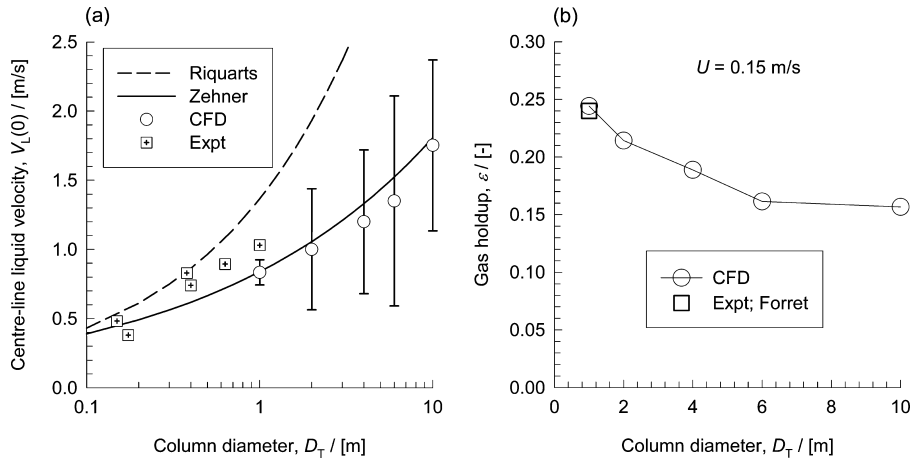

Figure 10. CFD simulation data on (a) centre-line liquid velocity $V_L(0)$ and (b) gas holdup ε as function of D_T for operation at $U = 0.15\,\mathrm{m\,s^{-1}}$ in columns of 1, 2, 4, 6 and 10 m diameter. The error bars in (a) represent the standard deviations of the transient $V_L(0)$ data presented in Figure 9, obtained from the data set after the time indicated by the arrow mark. The continuous lines in (a) represents the correlation of Zehner (1986) and Riquarts (1981). Also plotted in (a) are the experimental data of Forret *et al.* (2003) and Krishna *et al.* (1999a).

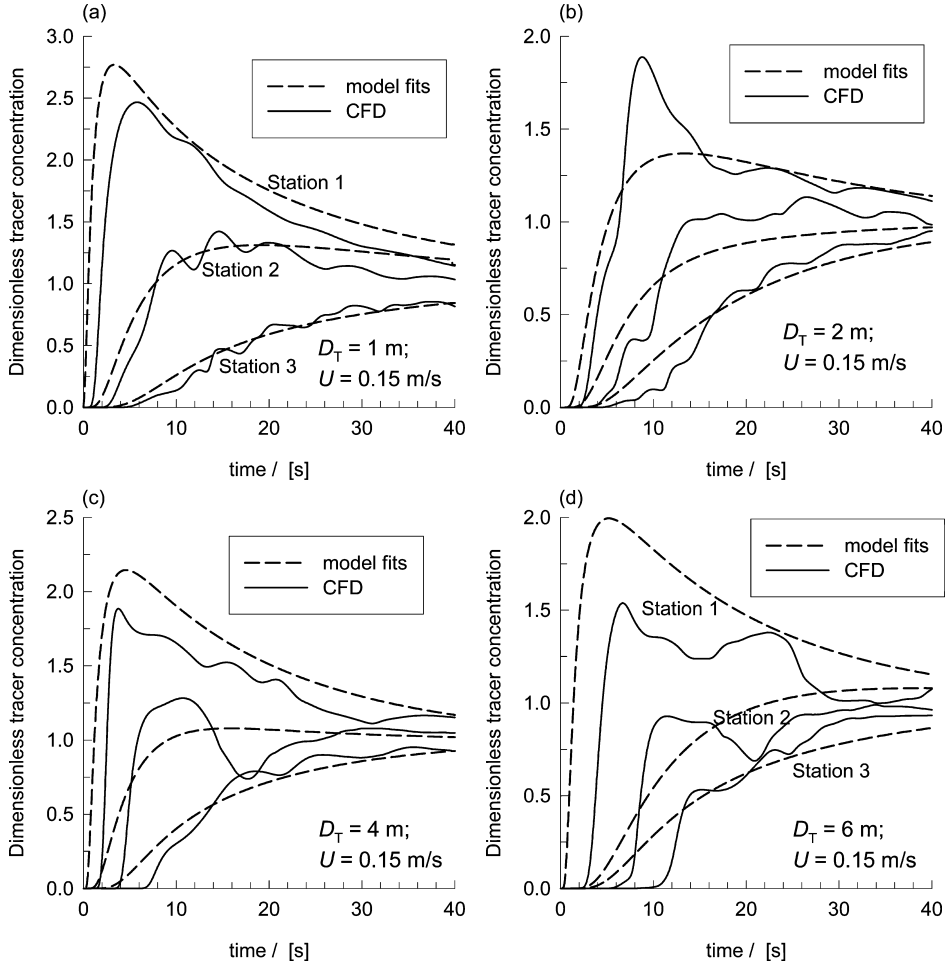

Figure 11. CFD simulations of the dimensionless liquid tracer concentration measured at three different monitoring stations for 1, 2, 4 and 6 m diameter columns operating at $U = 0.15\,\mathrm{m\,s^{-1}}$. The dashed lines represent the fits of the three simulation data sets using equation (9). Animations of liquid tracer dynamics are available on our web site: http://ct-cr4.chem.uva.nl/AWScaleUp/. (a–d) Liquid RTD in (a) 1 m column; (b) 2 m column; (c) 4 m column; (d) 6 m column.

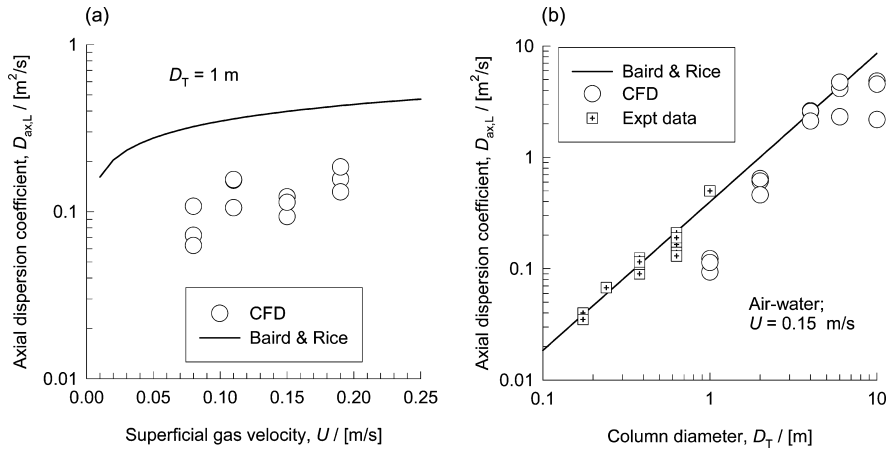

Figure 12. (a) Liquid phase axial dispersion $D_{ax,L}$ data obtained from CFD simulations of 1 m diameter column operating at $U = 0.08$, 0.11, 0.15 and 0.19 m s^{-1}. (b) $D_{ax,L}$ data from three-dimensional simulations for operation at $U = 0.15$ m s^{-1} in columns of 1, 2 4, 6, and 10 m diameters. The continuous lines in (a) and (b) represent the correlation of Baird and Rice (1975). Also plotted in (b) are the experimental data of $D_{ax,L}$ of Forret *et al.* (2003) and Krishna *et al.* (2000a).

the RTD of the small bubbles show a camel-hump shaped curve; this is due to the fact that the small bubbles are 'entrained' in the liquid phase and circulate around the column, moving with the liquid. From Figure 13 we note that with increasing column diameter the RTD of the small bubbles tends to become increasingly bi-modal. A portion of the gas tracer in the small bubbles travels up the column in the wake of the large bubbles, yielding a sharp first peak in the RTD curve. Another portion of the gas tracer ends up in the small bubbles that are entrained in the liquid phase; this yields a long tailing in the gas RTD.

Our CFD simulations therefore confirm this assumption, that has been suggested earlier in the literature (Krishna and Ellenberger, 1996; Krishna *et al.*, 1996) and used for simulation of the Fischer Tropsch slurry bubble column reactor (Maretto and Krishna, 1999). Gas phase tracer experiments of Vermeer and Krishna (1981) indeed show a camel hump in the gas phase RTD for operation in the heterogeneous flow regime. A camel-hump shaped curve is not amenable to interpretation in terms of an axial dispersion model and therefore we make no attempt to fit the CFD simulation results shown in Figure 13.

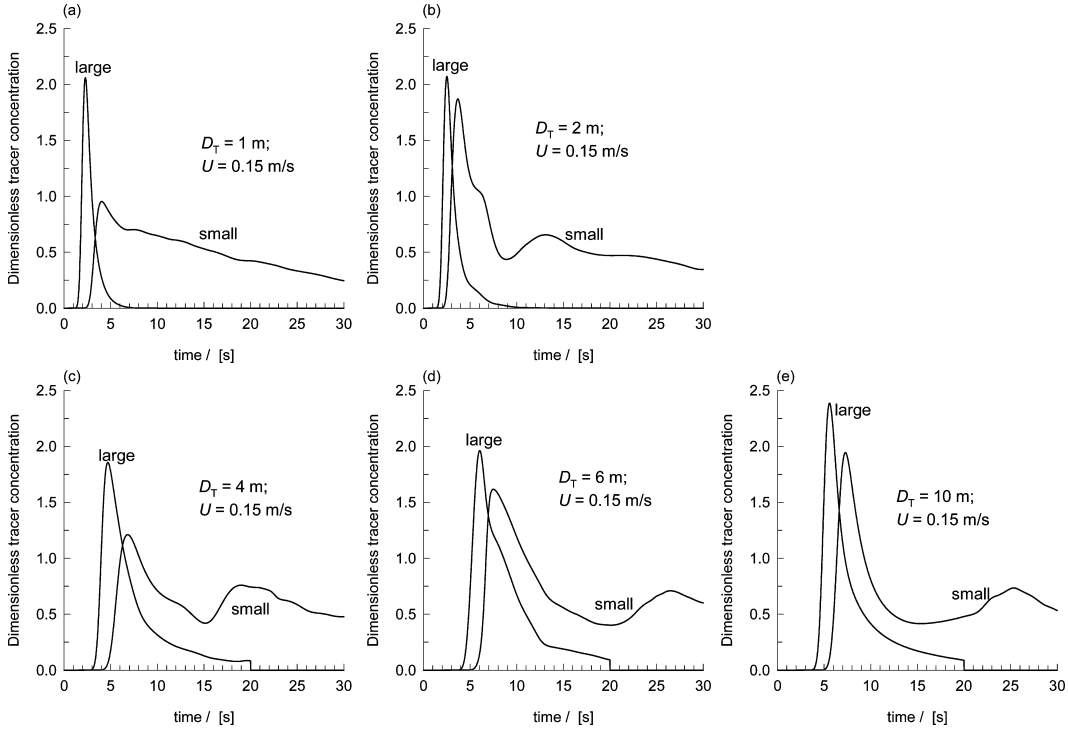

Figure 13. CFD simulations of the dimensionless tracer concentration in large bubble, and small bubble phases measured at monitoring station 1 for (a) 1, (b) 2, (c) 4, (d) 6 and (e) 10 m diameter columns operating at $U = 0.15$ m s^{-1}.

CONCLUSIONS

In this paper we have advocated the use of Eulerian simulations for obtaining information on the hydrodynamics of a bubble column reactor of diameters ranging from 1 to 10 m, operating in the heterogeneous flow regime. A particular feature of our approach is that we allow for two bubble classes: 'small' and 'large'. Each of these bubble phases exchanges momentum with the liquid phase, with its own drag coefficient. There is no interaction between the large and small bubble phases. The crucially important inputs concerning the drag coefficient C_D and the bubble diameter were estimated from air–water measurement data of bubble swarm velocity, for large and small bubbles separately, obtained in columns of relatively small scale, 0.1–0.38 m in diameter.

The following major conclusions can be drawn from this work.

(1) The three-dimensional transient simulations are able to reproduce the chaotic hydrodynamics observed visually and can yield reasonable values of $V_L(0)$ and $D_{ax,L}$ for the 1 m diameter reactor (Forret *et al.*, 2003).
(2) CFD simulations of bubble columns of 1, 2, 4, 6 and 10 m diameters show that the $V_L(0)$ values correspond very well with the Zehner (1986) correlation.
(3) The axial dispersion coefficient of the liquid phase, $D_{ax,L}$ determined from the CFD simulations show the same trends and order of magnitudes as that from the Baird and Rice (1975) correlation.
(4) Gas tracer injection studies show that the 'large' bubbles traverse the column with a much lower degree of dispersion than the 'small' bubbles. The small bubbles circulate along with the liquid phase, and as a first-order approximation their dispersion characteristics can be assumed to be the same as that of the liquid phase.

We conclude that Eulerian simulations can provide a powerful tool for hydrodynamic scale up of bubble columns, obviating the need for large scale experiments on gas holdup, liquid velocity and mixing. Validation of the proposed scale-up strategy is essential. The approach presented in this paper can also be applied to describe the influence of elevated pressures on the bubble column hydrodynamics (Krishna and van Baten, 2001a).

NOMENCLATURE

C_D	drag coefficient, dimensionless
C_L	liquid phase concentration, arbitrary units
d_b	diameter of bubble, m
$Đ_k$	diffusivity in phase k, $m^2 s^{-1}$
$D_{ax,L}$	liquid phase axial dispersion coefficient, $m^2 s^{-1}$
D_T	column diameter, m
g	gravitational acceleration, $m s^{-2}$
H_0	initial height of liquid in the column, m
H_{obs}	height at which the simulations are monitored (observed), m
H_T	total height of reactor, m
L_i	distance between tracer injection and monitoring, m
M	interphase momentum exchange term, $N m^{-3}$
n	index used in equation (9), dimensionless
p	system pressure, Pa
r	radial coordinate, m
t	time, s
u	velocity vector, $m s^{-1}$
U	superficial gas velocity, $m s^{-1}$
V_b	bubble swarm velocity, $m s^{-1}$
V_{b0}	bubble swarm velocity extrapolated to zero gas velocity, $m s^{-1}$
$V_L(r)$	radial distribution of liquid velocity, $m s^{-1}$
$V_L(0)$	centre-line liquid velocity, $m s^{-1}$

Greek symbols

ε	total gas hold-up, dimensionless
$\varepsilon(r)$	radial gas holdup profile, dimensionless
ε_k	holdup of phase k, dimensionless
μ	viscosity of fluid phase, Pa s
ρ	density of phase, $kg m^{-3}$
σ	surface tension of liquid phase, $N m^{-1}$

Subscripts

b	referring to bubbles (small or large)
eff	effective
G	referring to gas
L	referring to liquid
k, l	referring to phase k and l, respectively
trans	referring to transition velocity
T	tower or column

REFERENCES

Baird, M.H.I. and Rice, R.G., 1975, Axial dispersion in large unbaffled columns, *Chem Eng J*, 9: 171–174.

Clift, R., Grace, J.R. and Weber, M.E., 1978, *Bubbles, Drops and Particles* (Academic Press, San Diego, CA, USA).

Deckwer, W. D., 1992, *Bubble Column Reactors* (Wiley, New York, USA).

De Swart, J.W.A., van Vliet, R.E. and Krishna, R., 1996, Size, structure and dynamics of "large" bubbles in a two-dimensional slurry bubble column, *Chem Eng Sci*, 51: 4619–4629.

Forret, A., Schweitzer, J.-M., Gauthier, T., Krishna, R. and Schweich, D., 2003, Influence of scale on the hydrodynamics of bubble column reactors: an experimental study in columns of 0.1, 0.4 and 1 m diameters, *Chem Eng Sci*, 58: 719–724.

Hagesaether, L., Jakobsen, H.A. and Svendsen, H.F., 2002a, A model for turbulent binary breakup of dispersed fluid particles, *Chem Eng Sci*, 57: 3251–3267.

Hagesaether, L., Jakobsen, H.A. and Svendsen, H.F., 2002b, Modeling of the dispersed-phase size distribution in bubble columns, *Ind Eng Chem Res*, 41: 2560–2570.

Jakobsen, H.A., Sannaes, B.H., Grevskott, S. and Svendsen, H.F., 1997, Modeling of vertical bubble-driven flows, *Ind Eng Chem Res*, 36: 4050–4072.

Joshi, J.B., 2001, Computational flow modelling and design of bubble column reactors, *Chem Eng Sci*, 56: 5893–5933.

Koide, K., Morooka, S., Ueyama, K., Matsuura, A., Yamashita, F., Iwamoto, S., Kato, Y., Inoue, H., Shigeta, M., Suzuki, S. and Akehata, T., 1979, Behaviour of bubbles in large scale bubble column, *J Chem Eng Jpn*, 12: 98–104.

Kojima, E., Unno, H., Sato, Y., Chida, T., Imai, H., Endo, K., Inoue, I., Kobayashi, J., Kaji, H., Nakanishi, H. and Yamamoto, K., 1980, Liquid phase velocity in a 5.5 m diameter bubble column, *J Chem Eng Jpn*, 13: 16–21.

Krishna, R. and Ellenberger, J., 1996, Gas holdup in bubble column reactors operating in the churn-turbulent flow regime, *AIChE J*, 42: 2627–2634.

Krishna, R. and van Baten, J.M., 2001a, Eulerian simulations of bubble columns operating at elevated pressures in the churn turbulent flow regime, *Chem Eng Sci*, 56: 6249–6258.

Krishna, R. and van Baten, J.M., 2001b, Scaling up bubble column reactors with the aid of CFD, *Trans IChemE, Part A, Chem Eng Res Des*, 79: 283–309.

Krishna, R. and van Baten, J.M., 2002, Scaling up bubble column reactors with highly viscous liquid phase, *Chem Eng Technol*, 25: 1015–1020.

Krishna, R. and van Baten, J.M., 2003, Mass transfer in bubble columns, *Catal Today*, 79: 67–75.

Krishna, R., Ellenberger, J. and Sie, S.T., 1996, Reactor development for conversion of natural gas to liquid fuels: a scale-up strategy relying on hydrodynamic analogies, *Chem Eng Sci*, 51: 2041–2050.

Krishna, R., Urseanu, M.I., van Baten, J.M. and Ellenberger, J., 1999a, Influence of scale on the hydrodynamics of bubble columns operating in the churn-turbulent regime: experiments vs. Eulerian simulations, *Chem Eng Sci*, 54: 4903–4911.

Krishna, R., Urseanu, M.I., van Baten, J.M. and Ellenberger, J., 1999b, Wall effects on the rise of single gas bubbles in liquids, *Int Commun Heat Mass Transfer*, 26: 781–790.

Krishna, R., Urseanu, M.I., van Baten, J.M. and Ellenberger, J., 2000a, Liquid phase dispersion in bubble columns operating in the churn-turbulent flow regime, *Chem Eng J*, 78: 43–51.

Krishna, R., van Baten, J.M. and Urseanu, M.I., 2000b, Three-phase Eulerian simulations of bubble column reactors operating in the churn-turbulent regime: a scale up strategy, *Chem Eng Sci*, 55: 3275–3286.

Krishna, R., van Baten, J.M. and Urseanu, M.I., 2001, Scale effects on the hydrodynamics of bubble columns operating in the homogeneous flow regime, *Chem Eng Technol*, 24: 451–458.

Luo, H. and Svendsen, H.F., 1996, Theoretical model for drop and bubble breakup in turbulent dispersions. *AIChE J*, 42: 1225–1233.

Maretto, C. and Krishna, R., 1999, Modelling of a bubble column slurry reactor for Fischer-Tropsch synthesis, *Catal Today*, 52: 279–289.

Pan, Y., Dudukovic, M.P. and Chang, M., 1999, Dynamic simulation of bubbly flow in bubble columns, *Chem Eng Sci*, 54: 2481–2489.

Reilly, I.G., Scott, D.S., De Bruijn, T.J.W. and MacIntyre, D., 1994, The role of gas-phase momentum in determining gas holdup and hydrodynamic flow regimes in bubble-column operations, *Can J Chem Eng*, 72: 3–12.

Rhie, C.M. and Chow, W.L., 1983, Numerical study of the turbulent flow past an airfoil with trailing edge separation, *AIAA J*, 21: 1525–1532.

Riquarts, H.P., 1981, Strömungsprofile, Impulsaustausch und Durchmischung der flüssigen Phase in Bläsensaulen, *Chem Ing Techn*, 53: 60–61.

Sanyal, J., Vasquez, S., Roy, S. and Dudukovic, M.P., 1999, Numerical simulation of gas–liquid dynamics in cylindrical bubble column reactors, *Chem Eng Sci*, 54: 5071–5083.

Sokolichin, A. and Eigenberger, G., 1999, Applicability of the standard *k*–epsilon turbulence model to the dynamic simulation of bubble columns: Part I. Detailed numerical simulations, *Chem Eng Sci*, 54: 2273–2284.

van Baten, J.M. and Krishna, R., 2001, Eulerian simulations for determination of the axial dispersion of liquid and gas phases in bubble columns operating in the churn-turbulent regime, *Chem Eng Sci*, 56: 503–512.

van Doormal, J. and Raithby, G.D., 1984, Enhancement of the SIMPLE method for predicting incompressible flows, *Numer Heat Transfer*, 7: 147–163.

Vermeer, D.J. and Krishna, R., 1981, Hydrodynamics and mass transfer in bubble columns in operating in the churn-turbulent regime, *Ind Eng Chem Process Des Dev*, 20: 475–482.

Zehner, P., 1986, Momentum, mass and heat transfer in bubble columns. Part 1. Flow model of the bubble column and liquid velocities, *Int Chem Eng*, 26: 22–35.

ACKNOWLEDGEMENT

The Netherlands Organisation for Scientific Research (NWO) is gratefully acknowledged for providing financial assistance in the form of a 'programmasubsidie' for development of novel concepts in reactive separations technology.

The manuscript was received 12 November 2003 and accepted for publication after revision 15 April 2004.